Nuclear Instruments and Methods in Physics Research A 831 (2016) 349–354

Contents lists available at ScienceDirect

Nuclear Instruments and Methods in Physics Research A

journal homepage: www.elsevier.com/locate/nima

Aging and environmental tolerance of an optical transmitter for the ATLAS Phase-I upgrade at the LHC

F.X. Chang [a], H.T. Chang [b], T.S. Duh [c], T. Hayamizu [d], S. Hou [a,*], X. Hu [e], C. Liu [f], T. Liu [f], Y. Sakemi [d], T. Schwarz [e], P.K. Teng [a], P.R. Tsai [a], C.H. Wang [g], S.Y. Wang [b], Y. Yang [h], J. Ye [f]

[a] Academia Sinica, Taipei, Taiwan
[b] Liverage Technology Inc., Chupei, Taiwan
[c] Institute of Nuclear Energy Research, Longtan, Taiwan
[d] CYRIC, Tohoku University, Sendai, Japan
[e] Michigan University, Ann Arbor, MI, USA
[f] Southern Methodist University, Dallas, TX, USA
[g] National United University, Miaoli, Taiwan
[h] National Cheng Kung University, Tainan, Taiwan

ARTICLE INFO

Article history:
Received 20 November 2015
Received in revised form
8 April 2016
Accepted 11 April 2016
Available online 25 April 2016

Keywords:
Optical link
Radiation damage
Data transmission

ABSTRACT

The dual channel Miniature optical Transmitter (MTx) is developed for the ATLAS Phase-I upgrade requiring durable performance in the Large Hadron Collider environment. The data transmission has achieved 8 Gbps per channel with a custom-designed LOCld laser driver and 850 nm VCSELs packaged in transmitter optical sub-assemblies (TOSAs). The performance of the MTx opto-electronics is evaluated. Accelerated aging tests of the VCSELs were conducted in a chamber at 85 °C, 85% relative humidity, with TOSA and bare-die samples prepared in non-hermetic condition. Radiation tolerance of the VCSELs was investigated with 30 MeV and 70 MeV protons. The radiation induced effects in data transmission were investigated for light-power degradation and parameters of eye-diagrams.

1. Introduction

High speed optical transceivers are developed for readout of experiments at the Large Hadron Collider (LHC). Recent programs include a compact multi-channel transmitter designed for a new layer of the ATLAS pixel detector [1]. The Versatile Link project [2] provides several types of small form factor transceivers for Phase-I upgrades of LHC experiments in 2018. These modules are designed using radiation tolerant components in low-mass packaging.

The LHC in Phase-I will provide higher instantaneous luminosity of up to $3 \times 10^{34}/\text{cm}^2\,\text{s}$. The ATLAS upgrade is motivated to maintain an optimal trigger system by reduction of backgrounds and fakes [3]. In the following we discuss the dual channel Miniature optical Transmitter (MTx) [4] developed for the trigger electronics of the Liquid Argon (LAr) calorimeter [5] and the Muon New Small Wheel (NSW) spectrometer [6]. The MTx modules to be implemented in the LAr are required to withstand a total ionizing dose[1] of 0.3 kGy and a fluence of non-ionizing energy loss (NIEL) of 1×10^{13} (1 MeV) n/cm^2, for operation projected to an integrated luminosity of 3000 fb^{-1}. The NSW will employ FPGA-based router boards [8] to select and transmit data of triggered detector modules. The MTx's on the router boards will be installed on the detector outer rims, where the radiation field is an order of magnitude lower than in the calorimeter volume.

The MTx assembly being developed with a custom-designed LOCld laser driver capable of 8 Gbps per channel is described in Section 2. The type of laser diode chosen is the 850 nm Vertical-Cavity Surface-Emitting Laser (VCSEL) with light transmission through multi-mode fibers. Commercial VCSELs in bare-die and TOSA[2] package are evaluated for non-hermetic applications and radiation tolerance. Accelerated aging tests conducted in a control chamber at 85 °C, 85% relative humidity (RH) are discussed in Section 3. NIEL damages to VCSELs have been investigated with 30 MeV protons at INER [9] and 70 MeV protons at CYRIC [10]. In Section 4 we discuss the annealing of irradiated VCSELs, the light degradation as functions of proton fluences, and the eye-diagrams

* Corresponding author.

[1] Calculations in [7] scaled by safety factors of 2.25 for TID and 2.0 for NIEL.

[2] Transmitter Optical Sub-Assembly (TOSA), Lucent Connector (LC) packaged.

http://dx.doi.org/10.1016/j.nima.2016.04.033
0168-9002/

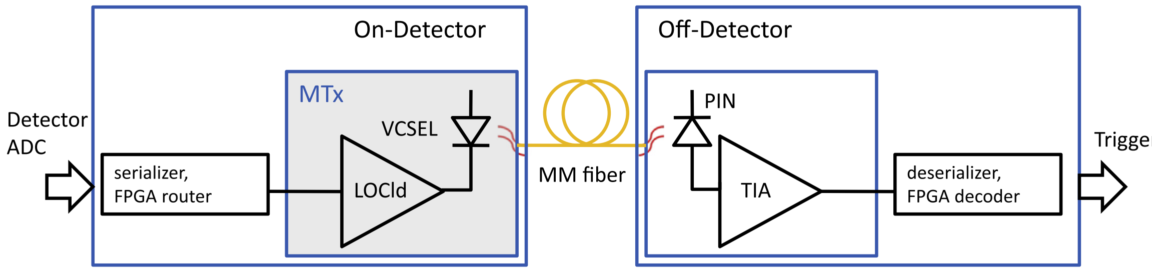

Fig. 1. Schematics of the optical links in the ATLAS Phase-I upgrade of LAr and NSW trigger electronics.

examined for 10 Gbps data transmission. A short summary is given in Section 5.

2. The MTx optical transmitter

The dual channel MTx is developed for applications in the ATLAS trigger data links, as illustrated in Fig. 1. The digitized detector signals are formatted by the custom-made serializer ASICs and are transmitted by the MTx modules. The NSW trigger bandwidth is optimized with router boards to select detector modules flagged for readout. The distance of data transfer from the on-detector MTx to the trigger processor is about hundred meters. For such a distance, the type of 850 nm oxide VCSELs is a good choice for being power-efficient and cost-effective.

The miniature form factor of the MTx is designed to fit in the limited enclosure for front-end electronics of the LAr calorimeter. The height of the MTx is specified to 6 mm maximum. A prototype module is shown in Fig. 2. The module has two 10 Gbps VCSELs packaged in TOSA format. The TOSAs are held in a latch, and are joined by a removable clip to ferrules mounted on the ends of multi-mode fibers. The TOSA packaging provides hermetically-sealed protection and precision alignment of light coupling to fiber in LC-type connector.

The laser driver of the MTx, called LOCld, is a custom-designed ASIC to convert electrical signals to laser current. It is fabricated by the 0.25 μm Silicon-on-Sapphire (SoS) CMOS technology, which is known for durable performance in radiation field. The prototypes were fabricated in single (LOCld1) and dual channels (LOCld2). The two separate channels in LOCld2 share auxiliary circuits for I^2C interface.

The speed of LOCld has achieved 8 Gbps in operation. A typical eye diagram of the MTx is shown in Fig. 3. The electrical inputs to the modules were transmitted from a pattern generator to provide 200 mV differential signals in a 2^7–1 pseudo-random bit sequence (PRBS), which repeated every 127 bits. The optical outputs were measured by a sampling oscilloscope.

The tolerance of the LOCld to ionizing dose was investigated by exposure to a X-ray source. The performance examined indicates no degradation in operation. The single event effects in radiation field were tested in neutron beams [11]. The bit-error-rate at 5 Gbps was less than 1×10^{-12} at the 95% confidence level. The results meet the ATLAS specification for applications in the Phase-I upgrade.

3. VCSEL reliability

The 850 nm GaAs-base oxide VCSELs contain typically a few quantum wells sandwiched between two multilayer mirrors of a total thickness of about 10 μm. The aperture of 10 Gpbs VCSEL is fabricated smaller to gain speed performance, and is considered more vulnerable to environmental factors. Although the newly

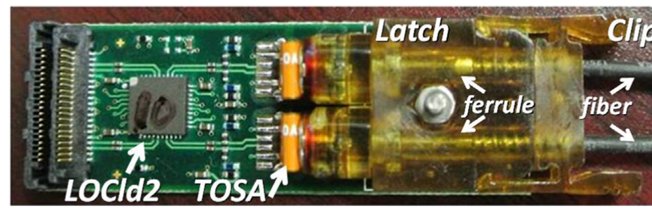

Fig. 2. A prototype MTx transmitter is shown. It has a custom developed LOCld2 driver (in QFN-40 package) and two TOSAs in a latch joined by a clip to LC-type ferrules on fiber ends.

developed VCSELs are demonstrated to be reliable for non-hermetic applications, catastrophic defects may occur due to electrostatic discharge events (ESD) or accidental power surge in handling.

Evaluation of 10 Gbps VCSELs of several manufacturers were conducted for the MTx use case in accelerated aging tests. The VCSEL samples were placed in an environmental chamber with the temperature kept at 85 °C and the relative humidity at 85%. The acceleration factor is given by the Arrhenius equation for thermally activated wear-out effects, and an empirically-determined exponential function for humidity induced corrosion [12]:

$$A = \exp((E_a/k_b)(T_{use}^{-1} - T_{acc}^{-1}))\cdot\exp(A_{RH}(RH_{acc} - RH_{use})),$$

where E_a=0.70 eV is the activation energy,[3] and k_b is the Boltzmann constant. The coefficient of relative humidity, $A_{RH} = 0.058\%^{-1}$, is suggested in [12]. The acceleration factor to operation at 30 °C and 50% RH is $A = 466$.

The VCSELs in aging tests were prepared in bare-die and TOSA formats at constant bias condition. Measurements were conducted after the VCSELs being cooled to room temperature. The light-power was measured by a large-area Ge photo-detector aligned in a jig on top of bare-die samples, or the end-face of a 12-fiber MT ferrule of fan-out fibers connecting TOSA samples. The photo-detector current was measured and calibrated by a light-power meter.

The aging tests had included VCSELs of types vulnerable to humidity, which lasted only a few hundred hours to failure. The TOSA samples, for being hermetically sealed, are good reference to demonstrate reliability in aging tests. The scan of light power versus laser current (*L–I*) was conducted by a PC-interface board to provide bias voltage and current. The *L–I* distributions of three types of TOSAs taken during burn-in are plotted in Fig. 4.

The type of bare-die VCSELs of the 10 Gbps TOSAs been tested were also investigated in the burn-in with the bias conditions of constant current (5 mA/ch) or voltage (2 V). The light-power measurements are plotted in Fig. 5, which are consistent over a period of 1500 h. The scaling of the acceleration factor suggests that the reliability is more than 10 years in room temperature operation.

[3] E_a=0.35 eV is given in Telcordia GR-468-Core [13]. E_a=0.7 eV or higher are suggested by manufacturers.

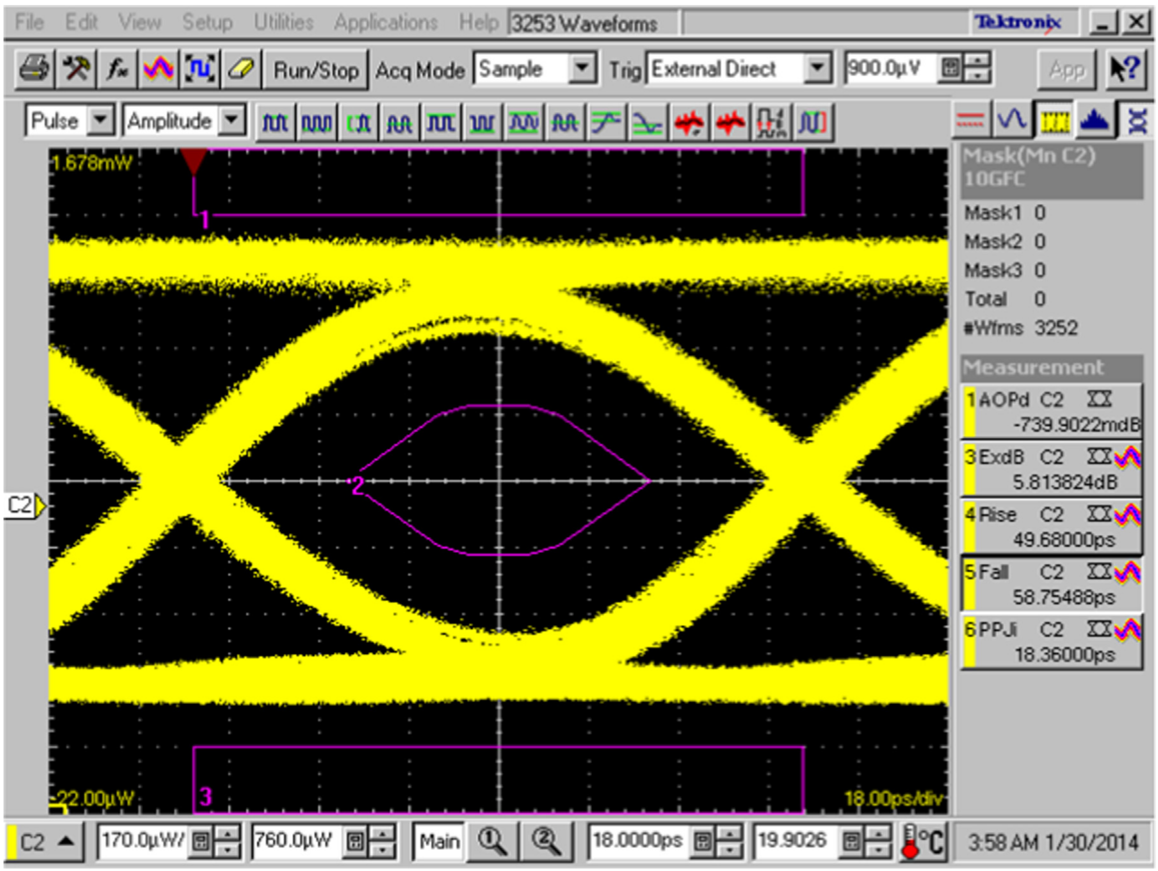

Fig. 3. Eye-diagram of a prototype MTx driven at 8 Gbps. The TOSA bias and modulation currents were set to 6.4 mA and 6 mA, respectively.

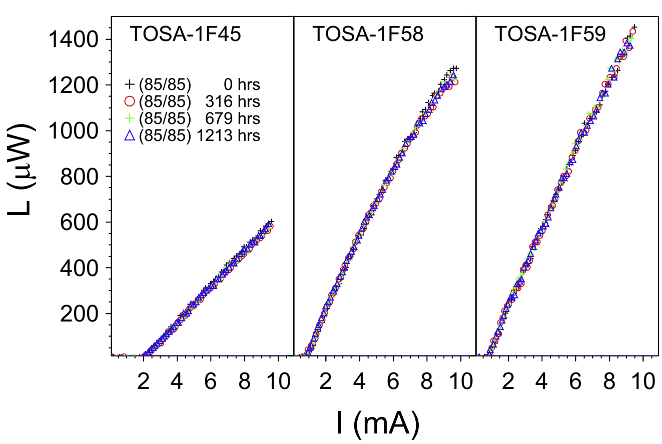

Fig. 4. The light-power distributions of three types of TOSAs (Truelight TTR-1F45 of 4.25 Gbps and TTR-1F58, TTR-1F59 of 10 Gbps) recorded before and during the 85 °C, 85% RH burn-in. The measurements were conducted in room temperature.

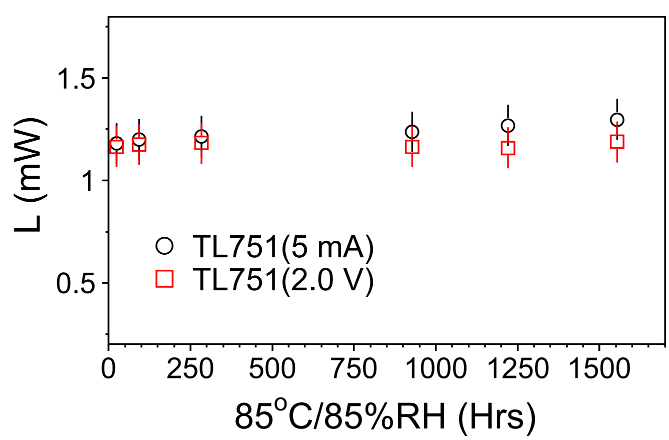

Fig. 5. The light power of bare-die VCSELs (Truelight TSD-8B12-751) measured during the 85 °C, 85% RH burn-in at bias conditions of constant current (5 mA/ch) or voltage (2 V). The measurements were conducted in room temperature.

4. Radiation tolerance of VCSELs

The radiation damages to VCSELs are observed for degradation of light-power with increasing threshold current. The damages can be partially annealed by charge injection in forward bias condition. The NIEL effects to VCSELs have been studied with 30 MeV protons at INER and 70 MeV protons at CYRIC. The beam fluxes were measured with a Faraday cup for beam currents and a two-dimensional gas chamber for beam profiles. The proton beams were delivered in Gaussian profiles with the RMS widths of a few millimeters, and the flux rates at the Gaussian centers of about 2×10^{10} p/cm^2 s and 2×10^{11} p/cm^2 s for 30 MeV and 70 MeV protons, respectively.

The test samples of bare-die VCSELs and TOSAs were prepared on circuit boards with the light emitting surface perpendicular to the beams and were irradiated passively channel by channel, each to the desired fluence. The annealing was then conducted with the VCSELs biased at the nominal forward current (6 mA).

The recovery of a 10 Gbps VCSEL in annealing is illustrated in Fig. 6 for the *L–I* measurements taken periodically. This sample had received a total fluence of 4.2×10^{14} (70 MeV) p/cm^2, which is equivalent to 2.8×10^{15} (1 MeV) n/cm^2 by scaling of the NIEL

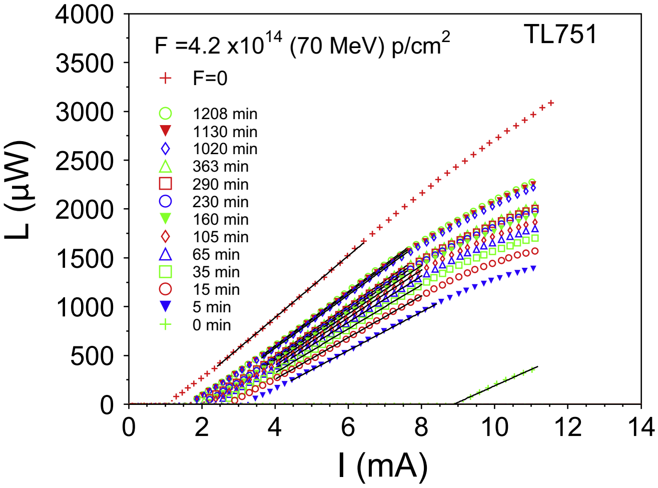

Fig. 6. The light-power distributions of a VCSEL (10 Gbps TSD-8B12-751) measured in annealing after a fluence of 4.2×10^{14} (70 MeV) p/cm^2. The annealing time accumulated in a forward bias of 6 mA is indicated for each *L–I* scan. The distribution taken prior to irradiation ($F=0$) is also plotted as reference.

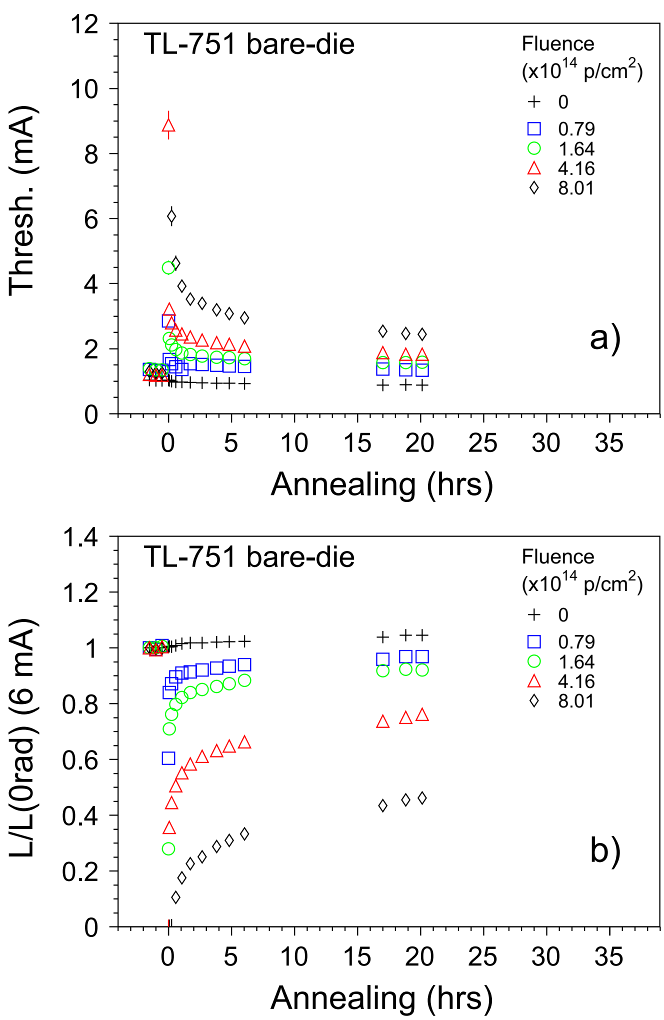

Fig. 7. The bare-die VCSELs (10 Gbps TSD-8B12-751) in annealing are plotted for (a) the threshold currents, and (b) the normalized light-power degradations at 6 mA. The distributions include four typical channels irradiated with the fluences of 70 MeV protons as indicated. A reference channel is also plotted to monitor fluctuations of systematic effects. Each data point is extracted from a linear fit to the corresponding *L–I* scan.

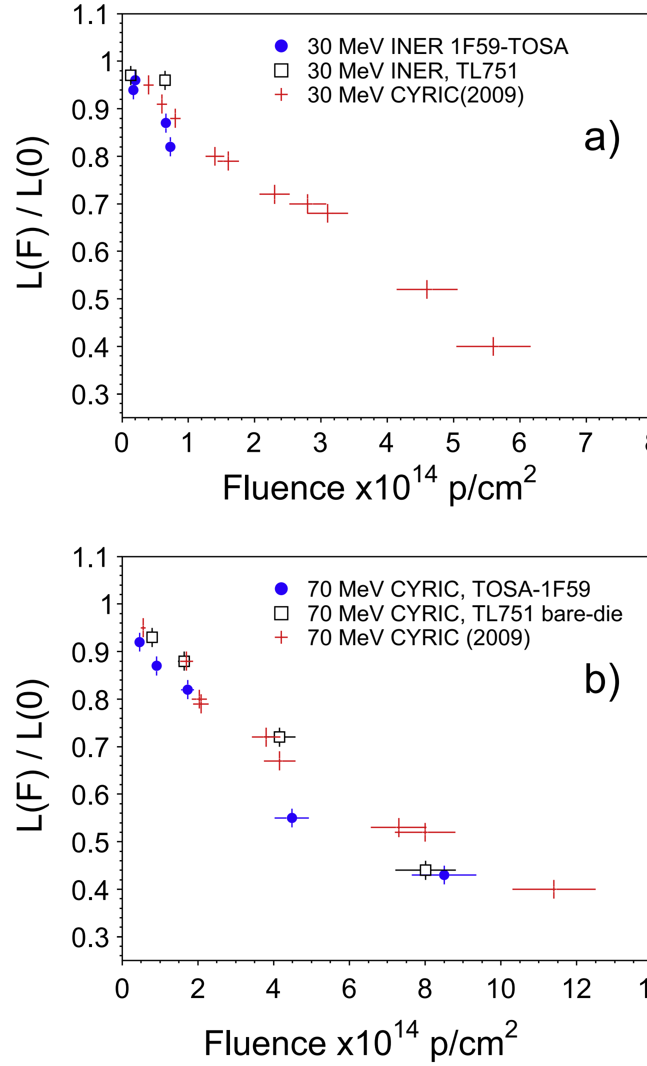

Fig. 8. The normalized VCSEL light power (after annealing) as functions of fluences in irradiation with (a) 30 MeV and (b) 70 MeV protons. The test samples include 10 Gbps VCSELs in bare-die and TOSA formats (Truelight TSD-8B12-751 and TTR-1F59 TOSA), and an earlier type (Truelight 2.5 Gbps TSA-8B12) reported in 2009 studies [17].

Table 1
Eye-diagrams of TOSA samples were examined on a 10 Gbps SFP+ test bench applying the same bias (6 mA) and modulation (8 mA) currents. The parameters obtained are listed for a reference channel and two of the irradiated with 30 MeV protons. The accumulated fluences are listed.

Fluence 10^{13} (p/cm^2)	0 (ref)	1.1	4.1
Optical power (dBm)	−0.11	−0.21	−0.61
Extinction ratio (dB)	4.6	4.81	4.92
Crossing (%)	47.9	46.6	46.0
Jitter peak-peak (mV)	17.5	15.5	18.7
Jitter RMS (mV)	2.47	2.35	2.92
Mask margin (%)	34	37	23
Rise time (pS)	37.5	37.5	36.4
Fall time (pS)	44.1	43.6	44.5
Op. Modu. Amp. (dBm)	−3.11	−3.08	−3.31

factors.[4] A linear fit was applied to each *L–I* scan to extrapolate the threshold current. The threshold current had increased to 9 mA

[4] The NIEL factors (keV cm^2/g) of GaAs: 0.55 for 1 MeV neutron, and 4.03, 3.64 for 30, 70 MeV protons, respectively [14].

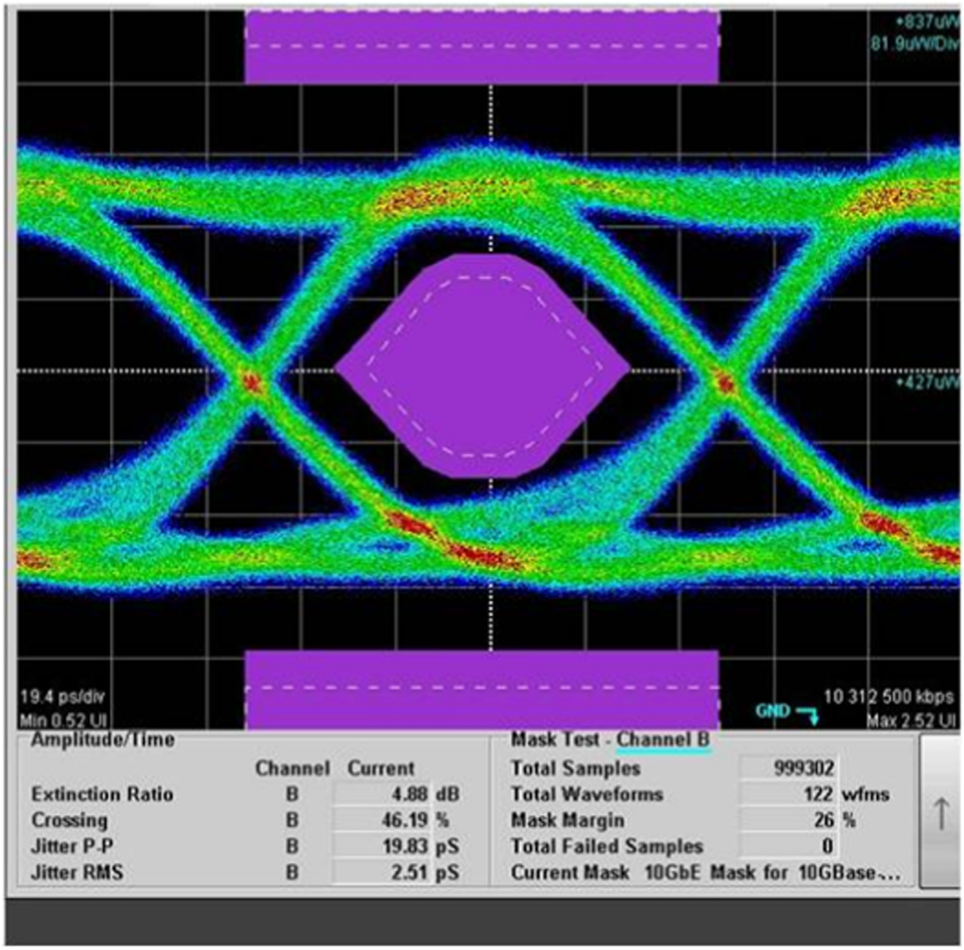

Fig. 9. Eye-diagram of an irradiated TOSA to a fluence of 4.4×10^{13} (30 MeV) p/cm^2. It was measured by a 10 Gbps SFP+ setup with the TOSA bias and modulation currents configured to 6 mA and 8 mA, respectively.

initially after irradiation. The quick recovery in annealing is observed with the threshold current reduced to less than 3 mA in a few minutes. The recovery is saturated after about a day, and the light power degradation at the nominal operation current is about 30% less than the value prior to irradiation (of $F=0$).

The recovery in annealing is approximately an exponential function in time. It is shown in Fig. 7 for the changes in threshold currents and the normalized light power at constant bias of 6 mA. The distributions are plotted for the VCSELs irradiated to various fluences, and a reference channel for monitoring fluctuations caused by deviations in room temperature and light coupling condition.

The NIEL effects in VCSELs are approximately linear to the fluence. It is shown in Fig. 8 for the light degradation of samples irradiated with 30 MeV and 70 MeV protons. The fractional loss per unit fluence is more severe with 30 MeV protons, by about 50% than with 70 MeV protons. This is consistent with the reported observations for GaAs devices [15], indicating that the damage coefficient does not follow the NIEL calculations [16].

The light degradations of TOSA samples are slightly higher than those of the bare-die VCSELs. It is partially due to the proton collisions in the TOSA packaging materials. As the proton beams were incident on the base of the TOSAs, secondary interactions caused more damages.

Measurements of previous studies for the first generation of oxide VCSELs [17] are also plotted in Fig. 8 for comparison. The 10 Gbps oxide VCSELs have similar epitaxial-structure as those of earlier products. The light degradations observed are compatible.

The radiation tolerance of the VCSELs is benefited by the thin device structure. For applications in the ATLAS upgrade, with the fluence of less than 1×10^{14} (1 MeV) n/cm^2, the light degradation suggested by results of the proton beam tests would be less than 10%.

The light degradation in VCSELs is not expected to effect their response characteristics. The 10 Gbps TOSA samples irradiated with 30 MeV protons were examined on a 10 Gbps SFP+ test bench with the TOSAs configured for the bias current of 6 mA and the modulation of 8 mA. Parameters obtained are listed in Table 1. The TOSAs have light power of around 600 μW and the eye-diagrams are compatible to those not irradiated. The eye-diagram of a TOSA being irradiated to 4.4×10^{13} (30 MeV) p/cm^2 is shown in Fig. 9.

5. Summary

The MTx optical transmitter is developed for the upgrade of the ATLAS LAr calorimeter and the NSW Muon Spectrometer. The miniature form factor of the module consists of a custom-developed LOCld laser driver, two 850 nm VCSELs packaged in TOSA format, and a custom made latching device for fiber connection. The LOCld is fabricated in SoS CMOS technology suitable for applications in radiation field. The TOSA package provides effective light coupling mechanism to fibers. The 850 nm oxide VCSELs of 10 Gbps were evaluated in accelerated aging tests. The NIEL effects were tested in proton beams. The light degradation corresponding to a fluence of 1×10^{14} (1 MeV) n/cm^2 is expected to be less than 10%. The lower light power can be corrected by increasing the laser modulation current. The MTx has the environmental tolerance required for applications in the ATLAS Phase-I upgrade with the data transmission of up to 8 Gbps.

References

[1] K.K. Gan, et al., J. Instrum. 10 (2015) C02018.
[2] J. Troska, et al., J. Instrum. 8 (2013) C12030.
[3] ATLAS Collaboration, CERN-LHCC-2011-011, LHCC-I-020, 2011.
[4] B. Deng, et al., IEEE Trans. Nucl. Sci. 62 (2015) 250.
[5] ATLAS Collaboration, CERN-LHCC-2013-017 and ATLAS-TDR-022, 2013.
[6] ATLAS Collaboration, CERN-LHCC-2013-006 and ATLAS-TDR-020, 2013.
[7] M. Dentan, P. Farthouat, ATLAS Policy on Radiation Tolerant Electronics, ATC-TE-QA-0001 (Rev. 2), 2000.
[8] J. Wang, et al., IEEE Trans. Nucl. Sci. 62 (2015) 2194.
[9] The TR30 Cyclotron at the Institute of Nuclear Energy Research (INER), Longtan, Taoyuan, Taiwan.
[10] The AVF 930 Cyclotron at the Cyclotron and Radioisotope Center (CYRIC), Tohoku University, Japan.
[11] X. Li, et al., J. Instrum. 10 (2015) C02017.
[12] R.W. Herrick, Reliability of fiber optic modules at Agilent technologies, in: Proceedings of IEEE 2002 Electronic Components and Technology Conference, 2002, p. 532.
[13] Generic Reliability Assurance Requirements for Optoelectronic Devices Used in Telecommunications Equipment, Telcordia GR-468-CORE, Issue 2, September 2004.
[14] G.P. Summers, et al., IEEE Trans. Nucl. Sci. 40 (1993) 1372.
[15] J.R. Srour, IEEE Trans. Nucl. Sci. 50 (2003) 653, and references therein.
[16] J.H. Warner et al., IEEE Trans. Nucl. Sci. 54 (2007) 1961, and references therein.
[17] S. Hou, et al., Nucl. Instrum. Methods Phys. Res. Sect. A 636 (2011) S137.